Hydrogen Bonding in 5-Bromouracil-Adenine-5-Bromouracil-Adenine (T^+AT^+A) Tetrads

Jiande Gu,*,† Jing Wang,‡ and Jerzy Leszczynski*,‡

Drug Design and Discovery Center, State Key Laboratory of Drug Research, Shanghai Institute of Materia Medica, Shanghai Institutes for Biological Sciences, Chinese Academy of Sciences, Shanghai 200031, People's Republic of China, and Computational Center for Molecular Structure and Interactions, Department of Chemistry, Jackson State University, Jackson, Mississippi 39217

Received: December 2, 2003; In Final Form: March 13, 2004

To understand the role of 5-bromouracil-adenine-5-bromouracil-adenine (T^+AT^+A) tetrads in the formation of tetraplexes, the relative stability of different conformers of the tetrad and their bonding characteristics have been studied by quantum chemistry methods. The influence of bromine in the formation of the T^+AT^+A tetrads has been revealed by comparative studies of thymine-adenine-thymine-adenine (TATA) and uracil-adenine-uracil-adenine (UAUA) tetrads. The stabilization energy of T^+AT^+A has been evaluated to be around 40 kcal/mol, comparable to those of TATA and UAUA. The role which the Br atom plays in the stabilization of the tetrads is 2-fold: by improving the proton-donating ability on its N3 position, it reinforces the H-bonding between A and T^+, while through electrostatic repulsion with N7 or N1 of A, it destabilizes the binding between the AT^+ pairs. The increase of the intra-base-pair binding energy compensates the decrease of the inter-base-pair interaction. This bifurcated H-bond consisting of $Br(T^+)$, $O4(T^+)$, and H6′(A) which binds two AT^+ pairs to form the stable T^+AT^+A tetrads has been revealed through the atoms-in-molecules (AIM) theory, the complementary method of electron-localization function (ELF), and the electron density difference analysis. The results of this study suggest that TATA might exist in the dimeric intermolecular tetraplexes formed from the 12-nucleotide repeat sequences from human telomeres.

Introduction

Telomeres are protein−DNA assemblies that stabilize the ends of chromosomes and prevent chromosomes from fusing with each other. The structures of four-stranded stretches of human telomere DNA have implications for the design of anticancer drugs.[1] The formation of Hoogsteen bonded guanine tetrads (G-tetrads) leads to four-stranded structures[1−7] in guanine-rich oligonucleotides.[7−10] It has been found that interactions with a metal ion are essential in the formation of G-tetrad complexes.[10−24] In addition to G-tetrad complexes, tetrads composed of other bases have also been determined by different experiments. The adenine tetrad (A-tetrad),[25] cytosine tetrad (C-tetrad),[26,27] and thymine tetrad (T-tetrad),[28,29] (also in RNA, uracil tetrad (U-tetrad)[30]) have been suggested by different NMR experiments. Guanine-cytosine-guanine-cytosine tetrads (GCGC) have been determined by crystallographic studies.[31−35] Also, a bowl-shaped tetrad structure in the presence of a potassium cation has been proposed for isoguanine by Tirumala and Davis[36] on the basis of NMR data. Recently, a new member of the base tetrad family has been obtained in the X-ray determination of the crystal structure of the dimeric intermolecular tetraplexes formed from 12-nucleotide repeat sequences from human telomeres.[37] Parkinson et al. observed that the two tetraplexes stack together through a pair of adenines in one tetraplex and a pair of thymines in the other, forming two stacked, symmetry-equivalent TATA tetrads. It has been suggested that such mixed tetrads might serve a valuable role in cells.[1]

Both the Watson−Crick type and Hoogsteen type TATA tetrads have been predicted to be stable in our previous quantum chemical study.[38] The stabilization energy has been calculated to be over 30 kcal/mol with the density functional theory for both conformers. However, the nonplanar structures of these two tetrads and the electrostatic potential analysis for the nonplanar structure suggest that it is unlikely to host a cation in their central area which seems to be inconsistent with what was observed in the crystallographic study of Parkinson et al.[37] However, it should be indicated that the DNA sequences used in their crystallographic study are $d(T^+AGGGT^+TAGGGT)$ in which T^+ is 5-bromouracil. Therefore, the observed TATA tetrad is in fact T^+AT^+A in which the methyl group of thymine has been replaced by bromine. To gain a better understanding of the role of T^+AT^+A in the formation of the tetraplexes, it is of importance to examine the influence of this group replacement on the tetrads' structures and properties. Quantum chemical studies of different base-tetrads have revealed that the stable tetrads play important roles in the formation of stable tetraplexes.[38−49] Also, to understand the diversity of the DNA tetraplexes, knowledge of the relative stability of different conformers of the tetrad and their bonding behavior is essential. The details of base-pairing patterns and their relation to the knowledge of relative stability of different conformers could only be revealed by accurate computational investigations. In this paper, the quantum chemistry studies of Watson−Crick type and Hoogsteen type T^+AT^+A tetrads and the corresponding base pairs are reported. The molecular geometries, the energy properties, the hydrogen bonding patterns, and the electrostatic potential characteristics involved in the formation of the tetrads are revealed. The influences of the substitution of the 5-methyl group of thymine by bromo on the structures and properties of

* Corresponding authors. E-mail: jerzy@ccmsi.us; jiandegush@go.com.
† Chinese Academy of Sciences.
‡ Jackson State University.

10.1021/jp0376830 CCC: $27.50
Published on Web 05/26/2004

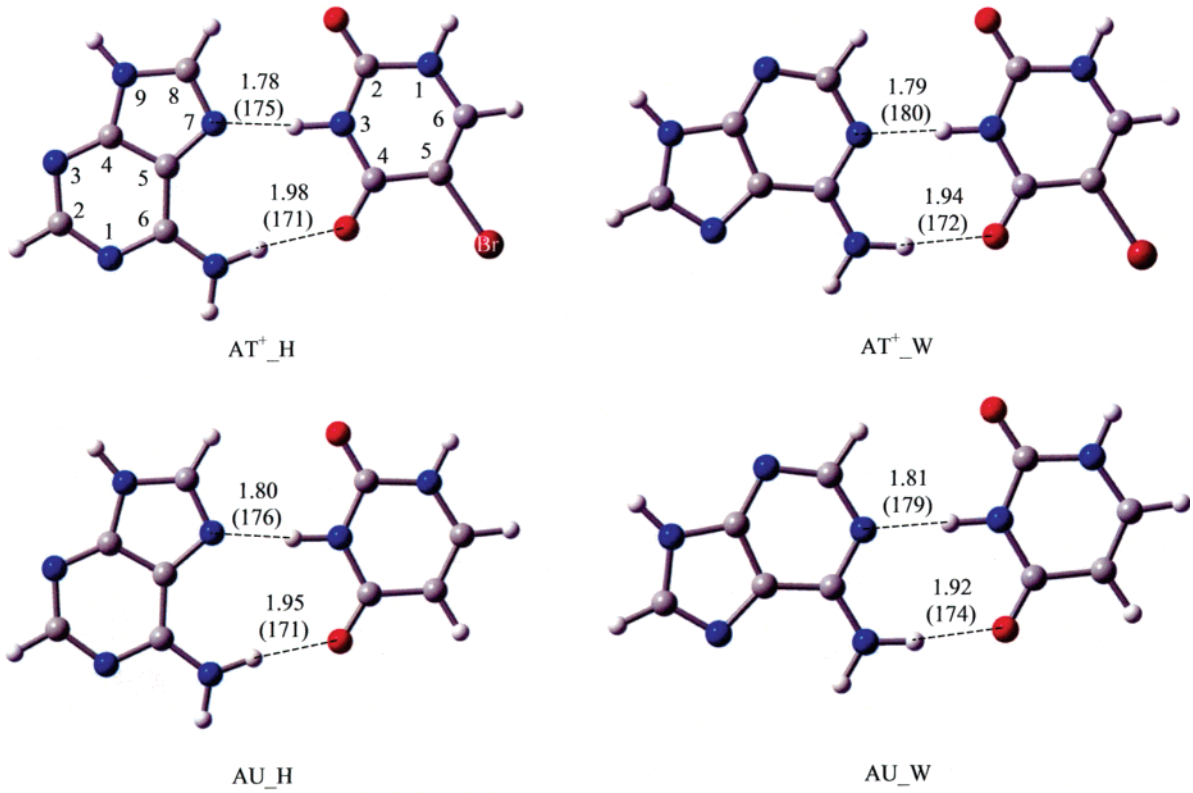

Figure 1. Optimized structures of AT^+ and AU base pairs along with the main geometric parameters. Numbers in parentheses are the bond angles in degrees. Atomic distances are in angstroms.

the tetrads are detailed. The corresponding studies of the uracil-adenine-uracil-adenine (UAUA) tetrads and the UA base pairs are also reported.

Method of Calculation

The local minima of the tetrad complexes have been fully optimized by analytic gradient techniques. No symmetry constraints were assumed during the optimization. The method used was the density functional theory (DFT) with Becke's three-parameter (B3)[50] exchange functional along with the Lee−Yang−Parr (LYP) nonlocal correlation functional (B3LYP).[51,52] The standard valence triple-ζ basis set augmented with *d*-type and *p*-type polarization functions, 6-311G(*d*,*p*),[53] was used. It is well-known that the geometries and frequencies of the molecules calculated at the B3LYP/6-311G(*d*,*p*) level agree well with experiment.[54] The absolute deviations for the bond lengths and angles at the B3LYP/6-311G(*d*,*p*) level are smaller than those at the MP2/6-31G(*d*) and QCISD/6-31G(*d*) levels of theory.[55] Our previous studies of hydrogen-bonded systems involving DNA bases have shown that the B3LYP approach predicts reliable interaction energies and is compatible with the MP2/6-31(*d*,*p*) method.[56,57] In the B3LYP/6-311G(d,p) level calculations of harmonic vibrational frequency, the force constants were determined analytically for all of the complexes. To analyze the H-bonding pattern in the tetrads, the atoms-in-molecules (AIM) theory of Bader[58,59] and a complementary method of the electron-localization function (ELF) by Becke and Edgecombe[60] and Silvi and Savin[61] were applied. The Gaussian-98 package of programs[62] was used in the calculations. The ELF calculations were performed by the TOPMOD package of programs.[63]

Results and Discussion

5-Bromouracil (T^+) Monomer and Adenine-5-Bromouracil (AT^+) and Adenine-Uracil (AU) Base Pairs. The optimized structures of the Watson−Crick type AT^+ pair (AT^+_W) and the Hoogsteen type AT^+ pair (AT^+_H) are similar to the corresponding AT base pairs that were predicted in our previous study of TATA tetrads.[38] The main geometric parameters are depicted in Figure 1. The H6(A)···O4(T^+) bond distance amounts to 1.94 and 1.98 Å for AT_W and AT^+_H, respectively, slightly longer than the corresponding bond distances in the AT pairs (1.93 Å for AT_W and 1.97 Å for AT_H). On the other hand, a slightly shorter N1(A)···H3(T^+) bond length of 1.79 Å is observed for AT^+_W compared to that of 1.83 Å in the AT_W pair. A similar short N7(A)···H3(T^+) bond length has also been detected for the Hoogsteen type AT^+ pair: 1.78 Å in AT^+_H and 1.80 Å in AT_H. The H-bonds in the optimized structures of AU base pairs (Figure 1) exhibit close similarity to those of the AT pairs. The H6(A)···O4(U) and the N1(A)···H3(U) bond distances are evaluated to be 1.92 and 1.81 Å for AU_W, and the H6(A)···O4(U) and the N7(A)···H3(U) bond lengths are calculated to be 1.95 and 1.80 Å for AU_H, respectively. Since all of the calculations were performed at the same level of theory (B3LYP/6-311G(d,p)), the changes in the H-bond distances suggest that the bromine substitution at the C5 position of thymine improves the proton-donating ability at its N3 position and, meanwhile, slightly impairs the tendency of accepting a proton at the O4 site. However, the H-bonding in the base pairs has little influence on C−Br bonding as revealed in the almost same C−Br bond length for the monomer (1.892 Å) and for the base pairs (1.892 Å).

The binding energy of the Watson−Crick type AT^+ pair amounts to 15.64 kcal/mol (Table 1), 0.55 kcal/mol larger than that of the AT_W pair (15.09 kcal/mol at the B3LYP/6-311G(*d*,*p*) level of theory).[38] A similar increase in binding energy is also predicted for the Hoogsteen type AT^+ pair, where the stabilization energy is 16.10 kcal/mol, about 0.42 kcal/mol

TABLE 1: Energy Property of AT and AU Base Pairs as Well as the Related Bases Predicted at the B3LYP/6-311G(*d,p*) Level of Theory[a]

species	E/hartrees	E_0/hartrees	ΔE/(kcal mol^{-1})	ΔE_0/(kcal mol^{-1})
A	−467.439 215	−467.327 571		
U	−414.934 617	−414.847 599		
T^+	−2988.469 551	−2988.392 646		
AT^+_W (C_s)	−3455.933 552	−3455.743 271	−15.64	−14.47
AT^+_H (C_s)	−3455.934 295	−3455.743 930	−16.10	−14.88
AU_W (C_s)	−882.398 178	−882.197 592	−15.28	−14.07
AU_H (C_s)	−882.398 985	−882.198 376	−15.78	−14.56

[a] E_0 and ΔE_0 are zero-point corrected. ΔE and ΔE_0 are the relative energies corresponding to the separated bases.

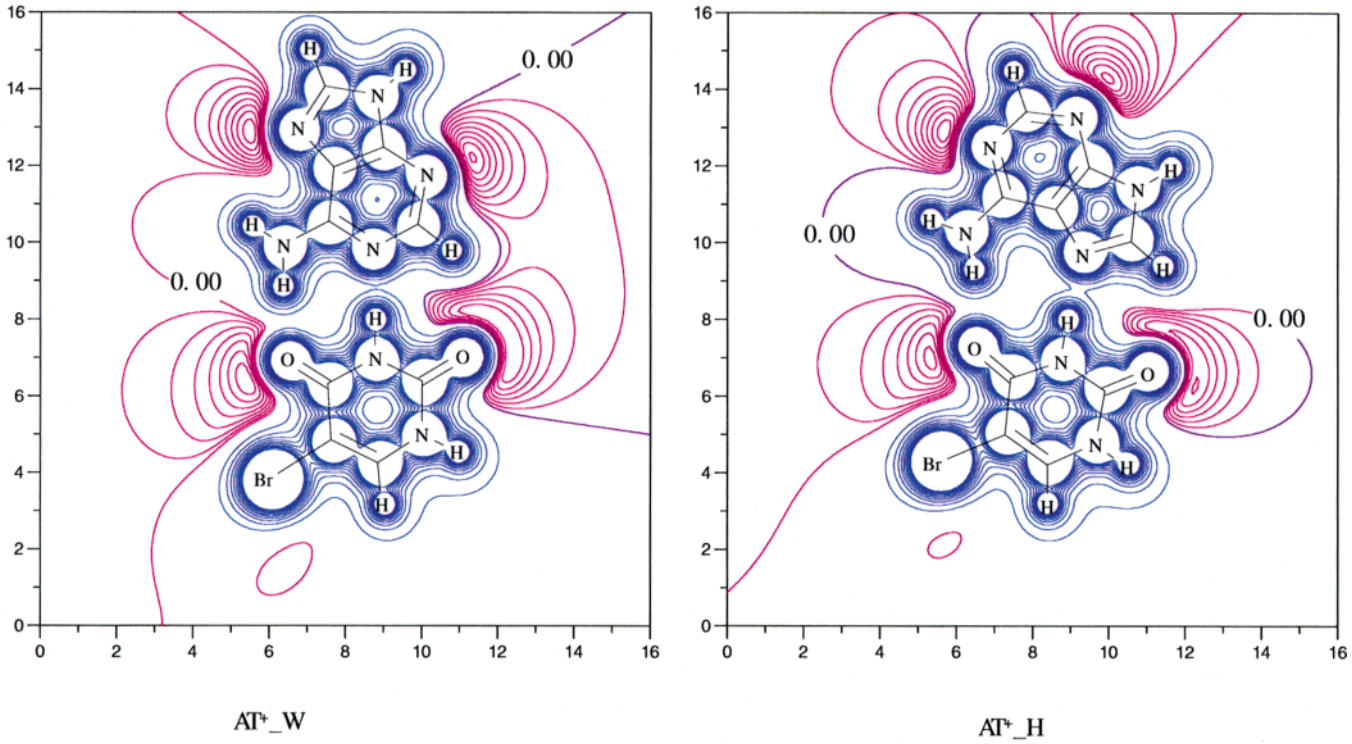

Figure 2. Electrostatic potential maps of AT^+ base pairs on the molecular plane. The blue line represents the positive part of the electrostatic potential, and the red line represents the negative part of the electrostatic potential. The contour spacing is 0.1 au for the positive part and 0.01 au for the negative part. The unit of the axes is angstroms.

higher than that of AT_H (15.68 kcal/mol).[38] The binding energies of the AU base pairs have been evaluated to be 15.28 kcal/mol for AU_W and 15.78 kcal/mol for AU_H, respectively, a little weaker than the corresponding AT^+ pairs. The increase in binding energy for the AT^+ pairs clearly suggests that the presence of Br at the C5 position of T^+ reinforces the hydrogen bonding between the bases.

Depicted in Figure 2 are the electrostatic potential maps of the AT^+ pairs. They are similar to those of the AT pairs.[38] However, the presence of Br enlarges the negative area around O4 and Br of 5-bromouracil and, therefore, from the viewpoint of electrostatic interactions, is expected to have negative effects on the formation of the tetrads.

T^+AT^+A Tetrads. Stationary points on the potential energy surface were located by the full optimization of the complexes. Although the nonplanar initial structures were assumed in the calculations, the geometry optimizations yielded only planar forms. Vibrational analysis reveals all real frequencies for both the Watson−Crick type (T^+AT^+A_W) and the Hoogsteen type (T^+AT^+A_H) tetrads and ensures that the stationary points are local energy minima. A significant difference compared with the TATA tetrads is that the T^+AT^+A tetrads are planar and possess C_{2h} symmetry. Two AT^+ base pairs are held together by bifurcated hydrogen bonding between the O4 of T^+s and the proton of the amino group of adenines (forming the O4-(T^+)···H6′(A) bond) not involved in the AT^+ pair bonding (Figure 3). Due to the second hydrogen bonding at the O4 position, the H6(A)···O4(T^+) bond distance increases to 2.00 Å for T^+AT^+A_W and 2.05 Å for T^+AT^+A_H, respectively. The elongation amounts to 0.05 Å for the former and 0.07 Å for the latter. The corresponding bond increase in the TATA tetrads has been found to be 0.10 and 0.07 Å, respectively. The second H-bonding on O4 of T^+ seems to be very weak in T^+-AT^+A_W; the O4(T^+)···H6′(A) bond distance has been computed to be 2.44 Å, about 0.41 Å larger than that in TATA_W. Even weaker O4(T^+)···H6′(A) bonding has been detected in T^+AT^+A_H in which the O4(T^+)···H6′(A) bond length amounts to 2.57 Å, about 0.53 Å larger than that in TATA_H. Nevertheless, relatively short atomic distances for Br(T^+)···H6′-(A) and Br(T^+)···N7(A) in T^+AT^+A_W (2.80 and 3.15 Å) and/or Br(T^+)···N1(A) in T^+AT^+A_H (2.82 and 3.20 Å) suggest that Br in T^+ might be involved in bonding either with the proton of the amino group of adenine or with N7(A) (or N1(A)). In the former case, H6′ of adenine is expected to be involved in the bifurcated H-bonds with both O4 and Br of T^+, resembling the well-known bifurcated H-bonding pattern found in the crystal structure of glycine[64] and in our previous study of GCGC tetrads.[45]

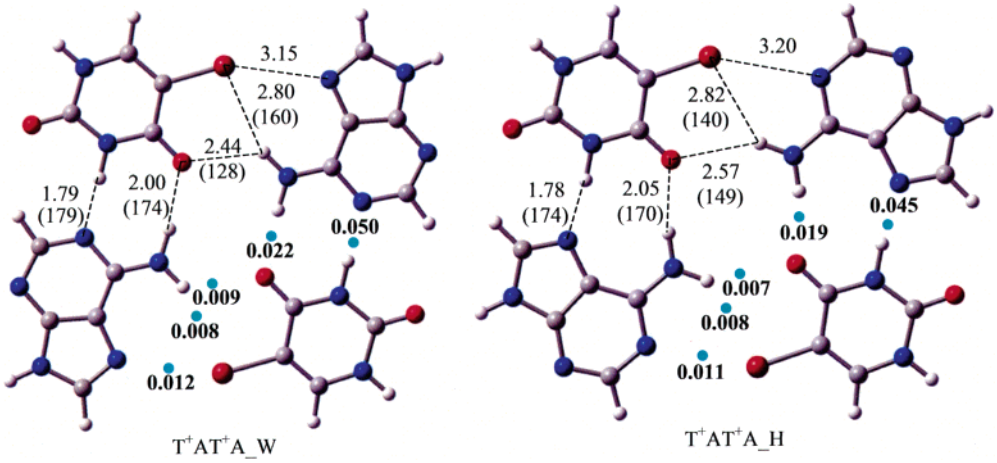

Figure 3. Optimized structures of the T^+AT^+A tetrads. Blue dots are the positions of the bond critical points by AIM analysis. The main geometric parameters and the density at the BCPs are listed. Numbers in parentheses are the bond angles in degrees. Atomic distances are in angstroms. Numbers in bold are the electron densities at the BCPs (au).

TABLE 2: Energy Property of T^+AT^+A and UAUA Tetrads Predicted at the B3LYP/6-311G(*d,p*) Level of Theory[a]

species	*E*/hartrees	E_0/hartrees	ΔE	ΔE_0	ΔE^p	$\Delta E_0{}^p$
$T^+AT^+A\_W$	−6911.881 034	−6911.499 527	−40.02	−37.08	−8.74	−8.15
$T^+AT^+A\_H$	−6911.880 636	−6911.498 988	−39.76	−36.74	−7.56	−6.98
UAUA_W	−1764.812 846	−1764.410 199	−40.90	−37.56	−10.35	−9.42
UAUA_H	−1764.816 862	−1764.413 866	−43.42	−39.86	−11.85	−10.74

[a] E_0 and ΔE_0 are zero-point corrected. ΔE and ΔE_0 are the relative energies corresponding to the separated bases. ΔE^p and $\Delta E_0{}^p$ are the relative energies corresponding to the separated base pairs. ΔE, ΔE_0, ΔE^p, and $\Delta E_0{}^p$ are in kcal/mol.

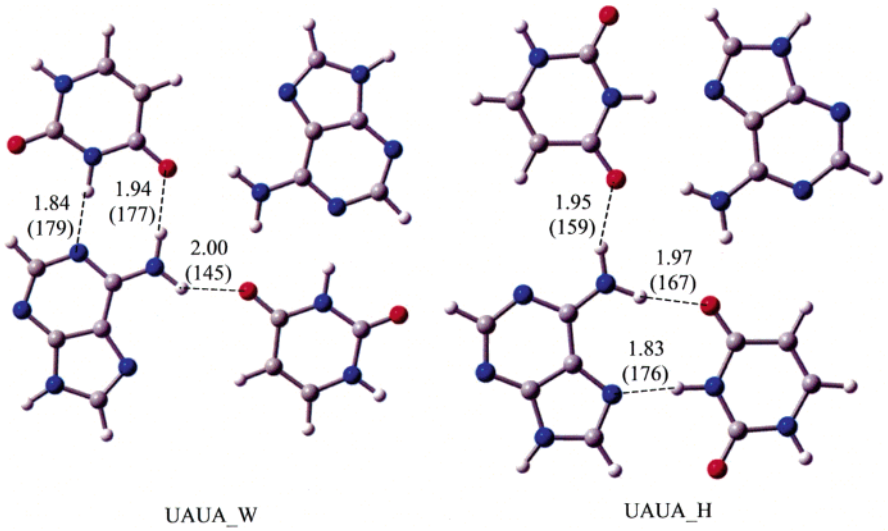

Figure 4. Optimized structures of the UAUA tetrads. Numbers in parentheses are the bond angles in degrees. Atomic distances are in angstroms.

The energy characteristics of the base pairs and the tetrads are summarized in Tables 1 and 2. The stabilization energy amounts to 40.02 kcal/mol for $T^+AT^+A\_W$ and 39.76 kcal/mol for $T^+AT^+A\_H$, respectively. These values are comparable to the stabilization energy of the TATA tetrads (without BSSE correction, they are 40.45 and 42.70 kcal/mol, respectively). The binding energy relative to the AT^+ base pairs of the T^+AT^+A tetrads has been evaluated to be 8.74 kcal/mol for the Watson−Crick type and 7.56 kcal/mol for the Hoogesteen type, respectively. For comparison, the corresponding binding energies of TATA tetrads are 10.26 kcal/mol for the former and 11.35 kcal/mol for the latter.[38] The fact that the binding energy of the T^+AT^+A tetrads is smaller than that of the TATA tetrads confirms the involvement of Br bonding in the formation of the tetrads. The interaction between Br and H′6(A) partly compensates for the energy losses of the weakened O4(T^+)···H6′(A) H-bonds and the Br···N7(A) (or N1(A)) electrostatic repulsion. Moreover, since the geometric characteristics of Br(T^+)···H6′(A) in $T^+AT^+A\_W$ (Br···H6′ atomic distance of 2.80 Å and N6H6′Br bond angle of 160°) are more in favor of H-bonding than those in $T^+AT^+A\_H$ (Br···H6′ atomic distance of 2.82 Å and N6H6′Br bond angle of 140°), a larger binding energy of $T^+AT^+A\_W$ implies the dominance of the Br(T^+)···H6′(A) type interaction.

Comparison with UAUA Tetrads. To explore the influence of Br of T^+ on the formation of the tetrads, UAUA tetrads without Br have also been studied at the same level of theory. The H-bonding patterns in UAUA are very close to those in the TATA tetrads (Figure 4). Specifically, the H6(A)···O4(U), N1(A)···H3(U), and O4(U′)···H6′(A) bond distances are evaluated to be 1.94, 1.84, and 2.00 Å for UAUA_W, and the H6(A)···O4(U), N7(A)···H3(U), and O4(U′)···H6′(A) bond

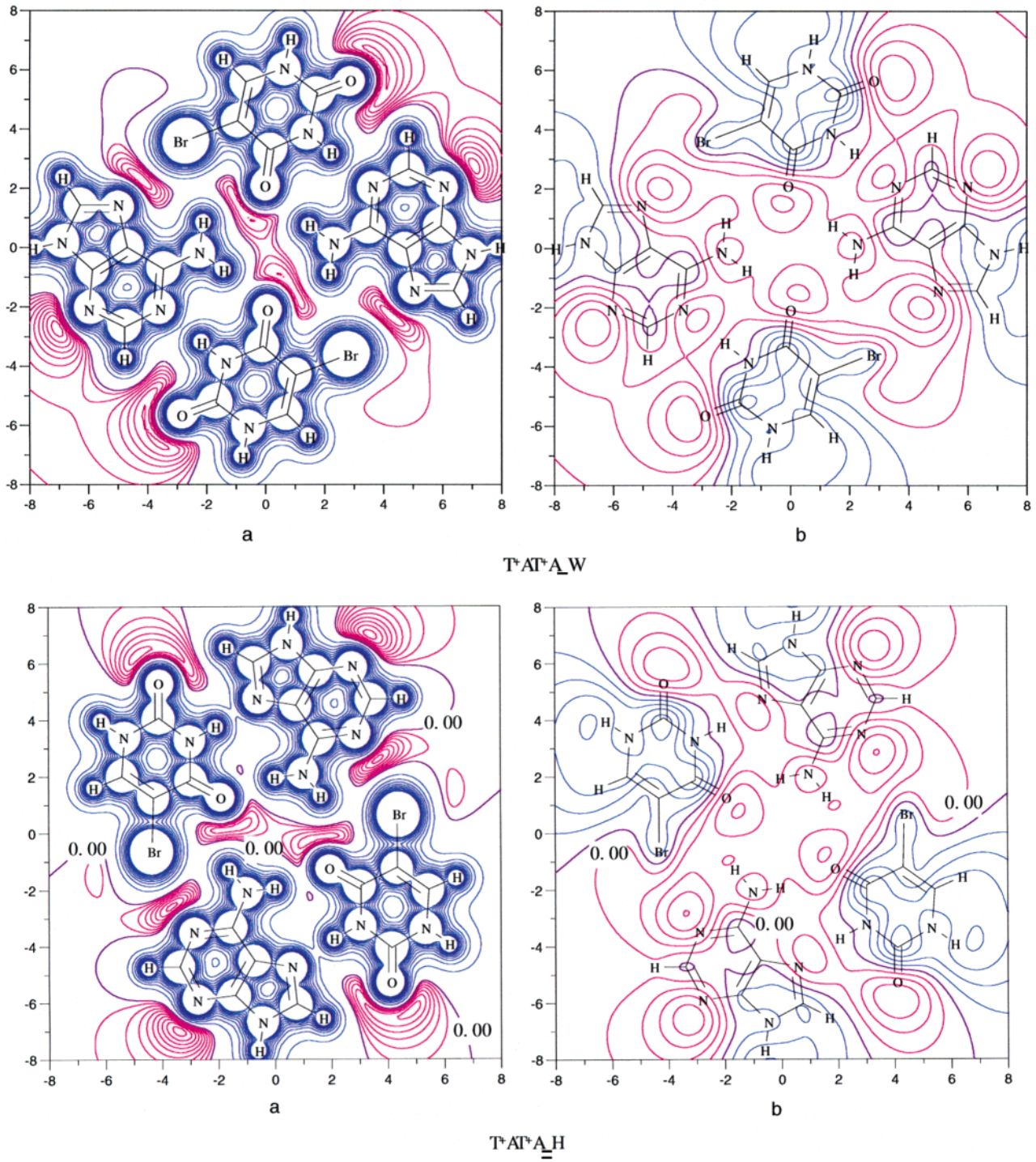

Figure 5. Electrostatic potential maps of the T^+AT^+A tetrads on the molecular plane (a) and 1.5 Å above the molecular plane (b). The blue line represents the positive part of electrostatic potential, and the red line represents the negative part of the electrostatic potential. The contour spacing is 0.1 au for the positive part and 0.01 au for the negative part in a. The contour spacing is 0.01 au for the positive part and 0.01 au for the negative part in b.The unit of the axes is angstroms.

lengths are calculated to be 1.97, 1.83, and 1.95 Å for UAUA_H, respectively. The planar (C_{2h}) structure for both the Watson−Crick type and Hoogsteen type UAUA tetrads optimized at the B3LYP/6-311G(*d,p*) level of theory has been proven to correspond to the transition state by subsequent vibrational analysis. The planar structures of T^+AT^+A should be the result of the involvement of bromine in the complexes. However, the small value of the imaginary frequency (*i*1 for UAUA_W and *i*6 for UAUA_H) found in the calculations indicates the negligible difference between the nonplanar and the planar conformer of UAUA. Little energy is needed to convert the UAUA tetrad from a nonplanar to a planar form. Consequently, TATA tetrads should also easily adopt the planar form under the influence of the surroundings.

The energy properties of UAUA tetrads are listed in Table 2. The binding energy between the UA pairs in UAUA tetrads is virtually the same as those in TATA tetrads (10.35 kcal/mol vs 10.26 kcal/mol for the Watson−Crick type and 11.89 kcal/mol vs 11.36 kcal/mol for the Hoogsteen type, respectively). The similarities of the H-bonding patterns and the binding energies for the UAUA and TATA tetrads justify the conclusion that the electrostatic repulsion between Br(T^+) and N7(A) (or

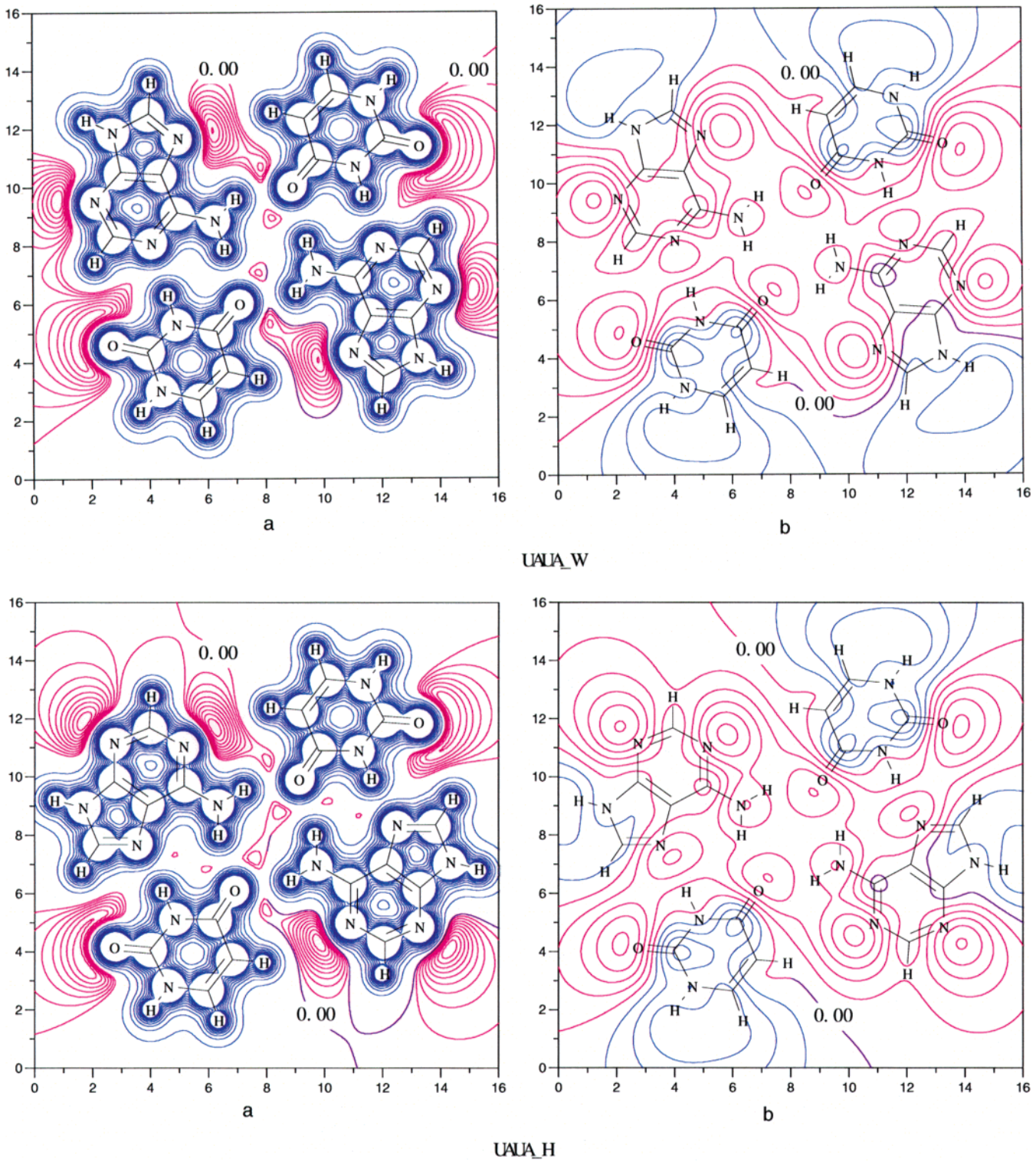

Figure 6. Electrostatic potential maps of the UAUA tetrads on the molecular plane (a) and 1.5 Å above the molecular plane (b). The blue line represents the positive part of the electrostatic potential, and the red line represents the negative part of the electrostatic potential. The contour spacing is 0.1 au for the positive part and 0.01 au for the negative part in a. The contour spacing is 0.01 au for the positive part and 0.01 au for the negative part in b.The unit of the axes is angstroms.

N1(A)) destabilizes the inter-base-pairs binding, and meanwhile the interaction between Br and H′6(A) partly compensates the energy losses of the weakened O4(T^+)···H6′(A) H-bonds.

Comparison with Crystal Structure. A comparison between the theoretical geometrical parameters and the available crystallographic data for the 12-mer tetraplex dimer is relevant to the estimation of the influence of environment such as the sugar−phosphate backbone on the structures and properties of the T^+AT^+A tetrad. Theoretical prediction of 3.15 Å for the N6(A)···O4($T^{+\prime}$) atomic distance is contained between the experimental values of 3.32 and 2.99 Å.[37] The distance of 4.15 Å between O4 of T^+ and the O4′ of the diagonal $T^{+\prime}$ evaluated by the DFT calculation is close to the corresponding value of 4.13 Å in the crystallographic data (PDB code 1k8p). Therefore, the inter-AT^+-base-pairs interaction seems not to be significantly affected by the surroundings. However, the interaction between

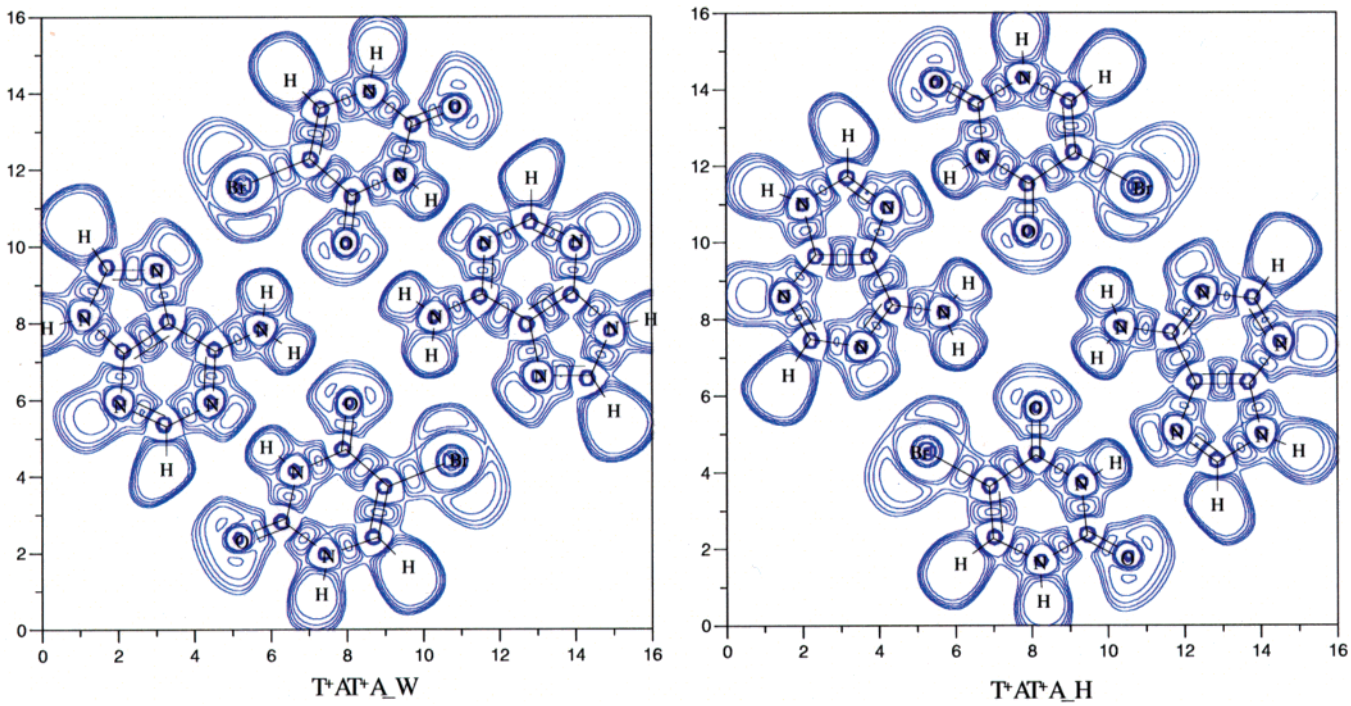

Figure 7. Electron density functions (ELF) on the molecular plane of the T^+AT^+A tetrads. The value of ELF ranges from 0.5 to 1.0 in the maps. The contour spacing is 0.1. The unit of the axes is angstroms.

A and T^+ within the AT^+ pair is much stronger in the isolated T^+AT^+A tetrad than in the tetraplex dimer. The N1(A)···N3-(T+) atomic distance in the isolated tetrad amounts to 2.48 Å, about 0.2 Å shorter than the corresponding crystallographical data (0.303 and 0.304 Å). The predicted N6(A)···O4(T^+) atomic distance (3.01 Å) is also shorter as compared to the 3.10 Å of experimental measurement.[37] Since no cations have been found around the T^+AT^+A tetrad core in the crystal structure, the reduced intra-AT^+-pair interactions might be attributed to the influence of the sugar−phosphate backbone.

Electrostatic Potential Maps of the Tetrads. The electrostatic potential (ESP) maps of T^+AT^+A and UAUA are depicted in Figures 5 and 6. From the ESP map 1.5 Å above the tetrads' plane, it is clear that the negative ESP above the center and the Br−N areas of the T^+AT^+A tetrads offers a good hosting position for the cations. Small cations such as Na^+ are expected to be sandwiched either between the stacked T^+AT^+A tetrads or between the stacked T^+AT^+A and GGGG tetrads. However, unlike the G-tetrad, in which the tetrad center allows the passing through of small cations, the narrow ESP negative area in the center of the tetrad plane is expected to block the pathway for cations. A comparison with the ESP maps of UAUA tetrads indicates that the UAUA tetrads can also be compatible hosts for cations. Therefore one can expect that TATA tetrads should also be good at accommodating cations when they adopt the planar form.

It is interesting to notice that, along the H-bonds H6(A)···O4(T^+) and N1(A)···H3(T^+), there is no sign change for the electrostatic potential of T^+AT^+A_W. This is also true along the line between Br and H6′(A). On the other hand, the electrostatic potential changes from positive to negative and to positive again along the weakened H-bond O4(T^+)···H6′(A). Since the H6(A)···O4(T^+) and N1(A)···H3(T^+) bonds are strong H-bonds, the similar electrostatic potential characteristics between Br and H6′(A) suggest a relatively strong bonding interaction. This is also true for T^+AT^+A_H. It is important that a similar phenomenon can also be seen from the electrostatic maps of other tetrads.[42,47,48]

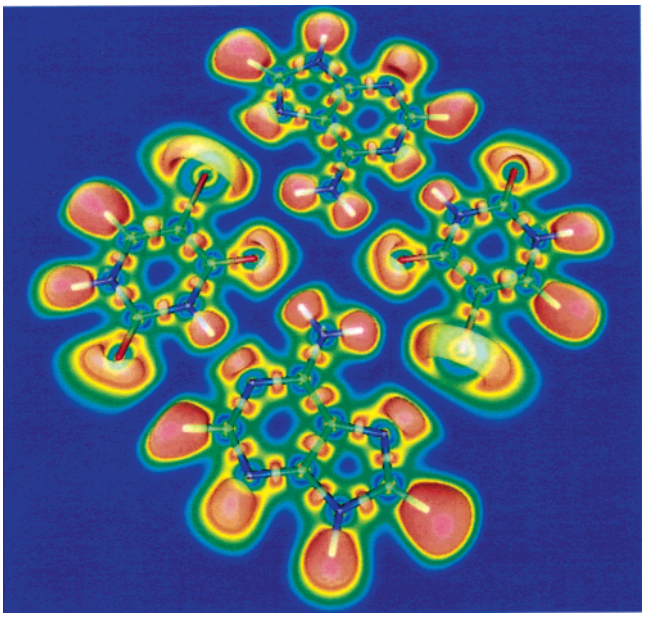

Figure 8. Three-dimensional representation of the ELF of T^+AT^+A_W. The ELF values: blue, 0.0; green, 0.5; yellow, 0.6; orange, 0.8. The three-dimensional parts are the isosurface with the ELF value of 0.85.

Bonding Patterns in T^+AT^+A Tetrads. The theory of AIM has been proven to be a useful and successful tool in the interpretation of charge density concerning a wide variety of chemical systems.[58,65,66] The density at the bond critical point (BCP) is of critical importance in AIM. It has been used to characterize different types of chemical bonds. It has been proposed that for H-bonding the density at BCP ranges between 0.002 and 0.035 au.[67] The AIM calculations in the present study were performed at the B3LYP/6-311G(*d*,*p*) level of theory. The charge densities of the BCPs of both types of T^+AT^+A tetrads have been depicted in Figure 3. The large values (0.022 and 0.050 au) of the density at the BCPs of the H6(A)···O4(T^+) and N1(A)···H3(T^+) bonds coincide with their short bond

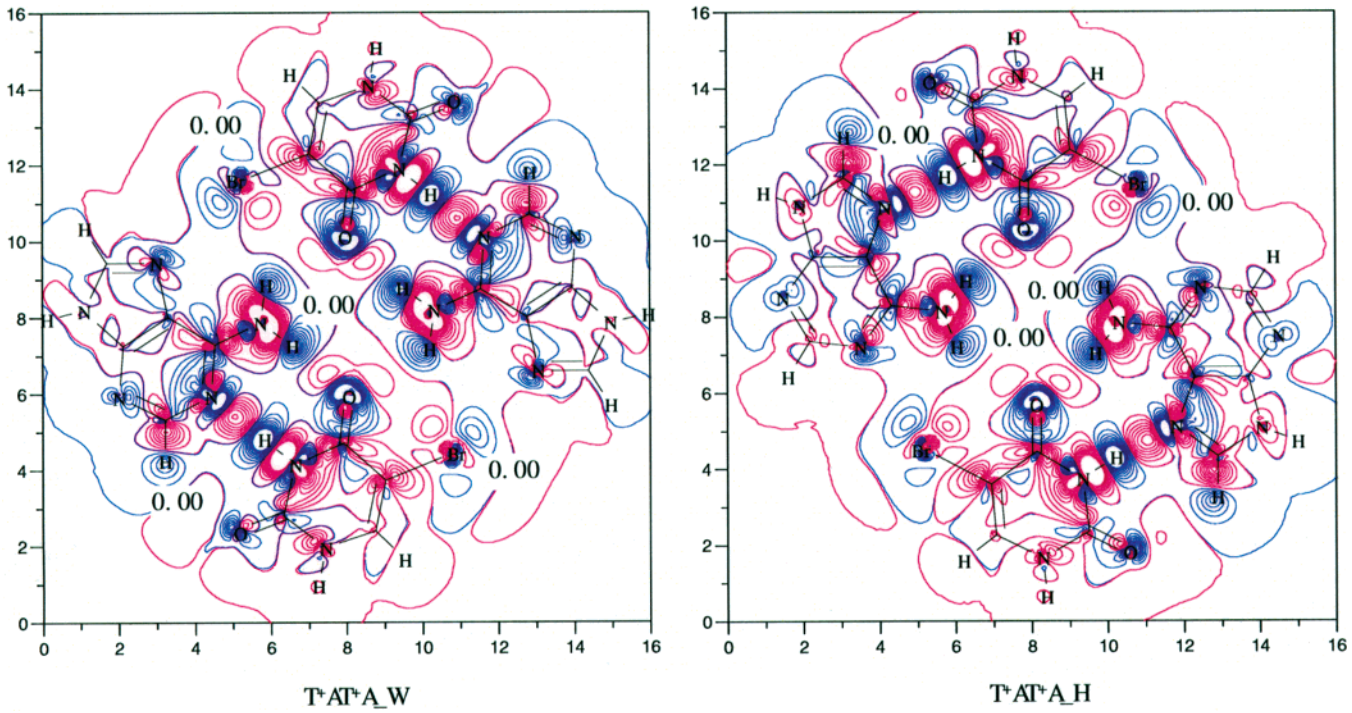

Figure 9. Electron density difference between the T^+AT^+A tetrad and the separated monomers on the molecular plane ($\Delta\rho = \rho(T^+AT^+A) - 2\rho(T^+) - 2\rho(A)$). The blue line represents a decrease in electron density, and the red line represents an increase in electron density in the formation of the tetrad. The contour spacing is 0.0008 au. The unit of the axes is angstroms.

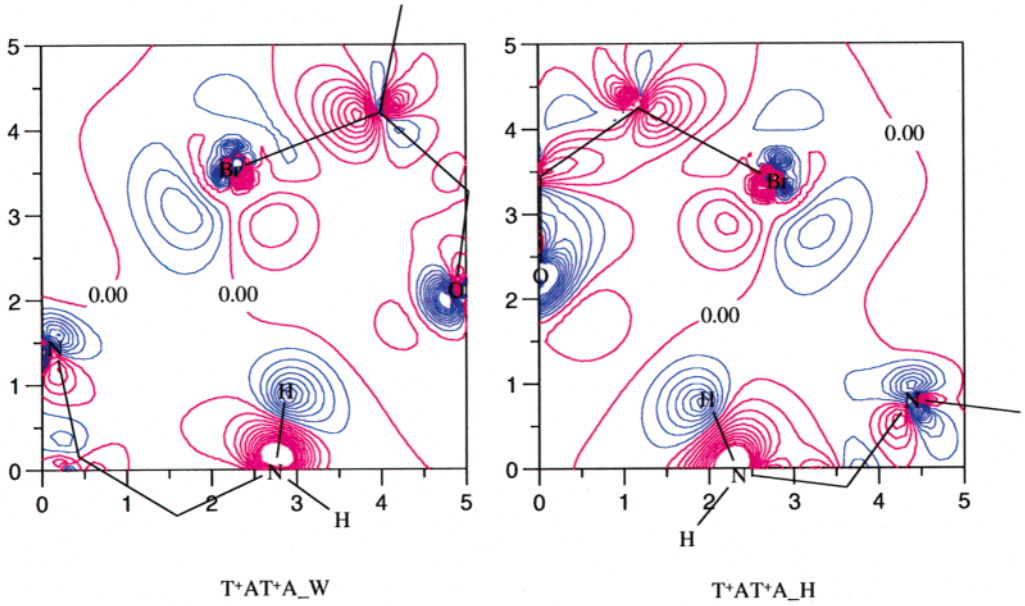

Figure 10. Electron density difference between the T^+AT^+A tetrad and the separated base pairs on the molecular plane around the $O4(T^+)$, $Br(T^+)$, N7(A), and H6′(A) atoms in $T^+AT^+A\_W$ and around the $O4(T^+)$, $Br(T^+)$, N1(A), and H6′(A) atoms in $T^+AT^+A\_H$ ($\Delta\rho = \rho(T^+AT^+A) - 2\rho(AT^+)$), The blue line represents a decrease in electron density, and the red line represents an increase in electron density in the formation of the tetrad. The contour spacing is 0.0008 au. The unit of the axes is angstroms.

lengths in $T^+AT^+A\_W$. The density of 0.009 au at the BCP of the $O4(T^+)\cdots H6'(A)$ bond signifies a very weak H-bond, although it still falls in the range considered by the criterion of the H-bond. The density at the BCP of $Br(T^+)\cdots H6'(A)$ amounts to 0.008 au and implies that the interaction energy of $Br(T^+)\cdots H6'(A)$ is almost the same as that of $O4(T^+)\cdots H6'(A)$. It is important to mention that there is also a BCP found between the N7 of A and the Br of T^+. Also, the value of the electron density (and the type of the BCP) falls into the range established by the criterion of the H-bond. The relatively larger density value of 0.012 at the BCP seems to suggest the stronger interaction between N7 and Br. Similar results can also be seen for $T^+AT^+A\_H$.

As a complementary method to study the bonding pattern among the $O4(T^+)$, $Br(T^+)$, N7(A), and H6′(A) atoms, the ELF analysis has been applied. According to the definition, ELF runs from 0 to 1 and equals 0.5 for the homogeneous electron gas.[60,61] Figure 7 displays the contour map of the ELF of the T^+AT^+A tetrads with values from 0.5 to 1.0. The well-localized electron function regions of $O4(T^+)$ and $Br(T^+)$ point to that of H6′(A), suggesting the bifurcated H-bond pattern for H6′(A). However, the well-localized area of N7(A) in $T^+AT^+A\_W$ (N1 in

T^+AT^+A_H) directs toward the nonlocalized zone of Br. From the 3-D presentation of the ELF of T^+AT^+A_W (Figure 8), it is clear that the localized area of N7(A) points to the hollow around the Br atom. One could expect no n-σ type interaction[67] between them.

The H-bonding can also be characterized by the electron density change for the bonded moiety. The electron densities around the proton and the proton acceptor decrease, while the density between the proton and its acceptor increases in the process of formation of the H-bond.[68] The electron density alteration from monomers to tetrad has been plotted for the two forms of the T^+AT^+A tetrad (Figure 9). The reduction of electron density at H3(T^+) and N1(A) or N7(A) and at O4(T^+) and H6(A) as well as the increase of the density between these two atoms well-characterizes the H-bonding of the AT^+ base pair. To examine the bonding between the AT^+ pairs in the tetrads, the electron density difference between the tetrads and the corresponding base pairs are depicted in Figure 10. The decrease of electron density at Br(T^+), O4(T^+), and H6′(A) and the increase of density between Br and H6′ as well as between O4 and H6′ clearly characterizes the bifurcated H-bonding pattern for Br(T^+), O4(T^+), and H6′(A). Since the electron density increases more in Br(T^+)···H6′(A) than in O4(T^+)···H6′(A), we predict that the H-bonding between Br(T^+) and H6′(A) is stronger. The interaction between Br and N7 or N1 can only be described as electrostatic repulsion due to the fact that electron density diminishes between these two atoms.

Conclusions

By applying reliable theoretical methods, this quantum chemical study enables us to derive the following conclusions.

1. The total binding energy of both forms of T^+AT^+A tetrads is almost the same as predicted for TATA or UAUA. On the basis of the predicted values of binding energy, all these three tetrads can exist. The stabilization energy could be as high as 40 kcal/ mol.

2. The role that Br atom plays in the stabilization of the tetrads is 2-fold: by improving the proton-donating ability at its N3 position, it reinforces the H-bonding between A and T^+, while through electrostatic repulsion with N7 or N1 of A, it destabilizes the binding between the AT^+ pairs. The increase of the intra-base-pair binding energy compensates for the decrease of the inter-base-pair interaction.

3. It is the presence of Br that forces planarity of the T^+AT^+A tetrads. The ESP of the tetrads suggests that the planar form could host small cations between two tetrads.

4. It is the bifurcated H-bond consisting of Br(T^+), O4(T^+), and H6′(A) that binds two AT^+ pairs to form the stable T^+AT^+A tetrads. The existence of this bifurcated H-bonding has been justified by the AIM theory, the ELF method, the ESP charateristics, and the electron density difference analysis.

5. This study indicates that TATA tetrads can easily adopt a planar form and, therefore, might exist in the dimeric intermolecular tetraplexes formed from the 12-nucleotide repeat sequences from human telomeres.

The results of this study could have biological relevance. The large binding energy (about 40 kcal/mol) of the T^+AT^+A tetrads ensures the formation of the stable dimeric intermolecular tetraplexes from the 12-nucleotide repeat sequences d(T^+AGGGT$^+$TAGGGT). Similar (or slightly larger) binding energies of UAUA and TATA are expected to stabilize the dimeric complexes. Vibrational frequency analysis for the UAUA tetrads reveals that the energy potential surface is very flat for the planar conformer. The ESP map of UAUA suggests a possible hosting position 1.5 Å above the tetrad plane. In this way, the tetrad will easily convert to a planar form under the influence of the stacking interaction with other tetrads and the electrostatic interaction with the intercalated cations. Because the geometrical characteristics and the bonding pattern of the TATA tetrads are similar to those of UAUA, one can expect that the bent form of the TATA tetrads can easily adopt a planar form when stacked between the guanine tetrads in the tetraplexes. A small cation such as Na^+ in the guanine tetraplexes could be sandwiched between the guanine tetrad and the planar form of TATA to increase the stability of the system. Consequently, the TATA tetrads might exist in the dimeric intermolecular tetraplexes formed from the 12-nucleotide repeat sequences from human telomeres.

Acknowledgment. This research project in the PRC was supported by the "Knowledge Innovation Program" and the "Introducing Outstanding Overseas Scientists Project", Chinese Academy of Sciences. In the USA the project was supported by ONR Grant No. N00034-03-1-0116, NIH Grant No. G1 2RR13459-21, NIH SCORE Grant 3-S06 GM008047 31S1, and NSF CREST Grant No. HRD-0318519.

References and Notes

(1) Patel, D. J. *Nature* **2002**, *417*, 807−808.
(2) Sasisekharan, V.; Zimmermann, S. B.; Davies, D. R. *J. Mol. Biol.* **1975**, *92*, 171−179.
(3) Pinnavaia, T. J.; Miles, H. P.; Becker, E. D. *J. Am. Chem. Soc.* **1975**, *97*, 7198−7200.
(4) Henderson, E.; Hardin, C. C.; Walk, S. K.; Tinoco, I., Jr.; Blackburn, E. H. *Cell* **1987**, *51*, 899−908.
(5) Williamson, J. R.; Raghuraman, M. K.; Cech, T. R. *Cell* **1989**, *59*, 871−880.
(6) Sen, D.; Gilbert, W. *Nature (London)* **1988**, *334*, 364−366.
(7) Blackburn, E. H.; Szostak, J. W. *Annu. Rev. Biochem.* **1984**, *53*, 163−194.
(8) Blackburn, E. H. *Annu. Rev. Biochem.* **1992**, *61*, 113−129.
(9) Blackburn, E. H. *Nature (London)* **1991**, *350*, 569−573.
(10) Henderson, E. R.; Blackburn, E. H. *Mol. Cell. Biol.* **1989**, *9*, 345−348.
(11) Ross, W. S.; Hardin, C. C. *J. Am. Chem. Soc.* **1994**, *116*, 6070−6080.
(12) Tohl, J.; Eimer, W. *Biophys. Chem.* **1997**, *67*, 177−186.
(13) Guschlbauer, W.; Chantot, J. F.; Thiele, D. *J. Biomol. Struct. Dyn.* **1990**, *8*, 491−511.
(14) Darlow, J. M.; Leach, D. R. F. *J. Mol. Biol.* **1998**, *275*, 3−16.
(15) Harrington, C.; Lan, Y.; Akman, S. A. *J. Biol. Chem.* **1997**, *272*, 24631−24636.
(16) Laughlan, G.; Murchie, A. I. H.; Norman, D. G.; Moore, M. H.; Moody, P. C. E.; Lilley, D. M. J.; Luisi, B. *Science* **1994**, *265*, 520−524.
(17) Phillips, K.; Dauter, Z.; Murchie, A. I. H.; Lilley, D. M.; Luisi, B. *J. Mol. Biol.* **1997**, *273*, 171−182.
(18) Nagesh, N.; Chatterji, D. *J. Biochem. Biophys. Methods* **1995**, *30*, 1−8.
(19) Kang, C.; Zhang, X.; Moyzis, R.; Rich, A. *Nature (London)* **1992**, *356*, 126−131.
(20) Hud, N. V.; Schultze, P.; Sklenar, V.; Feigon, J. *J. Mol. Biol.* **1999**, *285*, 233−243.
(21) Hud, N. V.; Schultze, P.; Feigon, J. *J. Am. Chem. Soc.* **1998**, *120*, 6403−6404.
(22) Mariani, P.; Mazabard, D.; Garbesi, A.; Spada, G. P. *J. Am. Chem. Soc.* **1989**, *111*, 6369−6373.
(23) Forman, S. L.; Fettinger, J. C.; Pieraccini, S.; Gottarelli, G.; Davis, J. T. *J. Am. Chem. Soc.* **2000**, *122*, 4060−4067.
(24) Marlow, A. L.; Mezzina, E.; Spada, G. P.; Masiero, S.; Davis, J. T.; Gottarelli, G. *J. Org. Chem.* **1999**, *64*, 5116−5129.
(25) Patel, P. K.; Koti, A. S. R.; Hosur, R. V. *Nucleic Acids Res.* **1999**, *27*, 3836−3843.
(26) Patel, P. K.; Bhavesh, N. S.; Hosur, R. V. *Biochem. Biophys. Res. Commun.* **2000**, *278*, 833−838.
(27) Patel, P. K.; Bhavesh, N. S.; Hosur, R. V. *Biochem. Biophys. Res. Commun.* **2000**, *270*, 967−971.
(28) Sarnam, M. H.; Luo, J.; Umemoto, K.; Yuan, R.; Sarma, R. H. *J. Biomol. Struct. Dyn.* **1992**, *9*, 1131−1153.
(29) Patel, P. K.; Hosur, R. V. *Nucleic Acids Res.* **1999**, *27*, 2457−2464.

(30) Cheong, C.; Moore, P. B. *Biochemistry* **1992**, *31*, 8406−8414.
(31) Metzger, S.; Lippert, B. *J. Am. Chem. Soc*. **1996**, *118*, 12467−12468.
(32) Kettani, A.; Kumar, R. A.; Patel, D. J. *J. Mol. Biol.* **1995**, *254*, 638−656.
(33) Darlow, J. M.; Leach, D. R. F. *J. Mol. Biol*. **1998**, *275*, 3−16.
(34) Kettani, A.; Bouaziz, S.; Gorin, A.; Zhao, H.; Jones, R. A.; Patel, D. J. *J. Mol. Biol*. **1998**, *282*, 619−636.
(35) Leonard, G. A.; Zhang, S.; Peterson, M. R.; Harrop, S. J.; Helliwell, J. R.; Cruse, W. B. T.; Langlois, d'Estaintot B.; Kennard, O.; Grown, T.; Hunter, W. N. *Structure* **1995**, *3*, 335−340.
(36) Tirumala, S.; Davis, J. T. *J. Am. Chem. Soc*. **1997**, *119*, 2769−2776.
(37) Parkinson, G. N.; Lee, M. P. H.; Neidle, S. *Nature (London)* **2002**, *417*, 876−880.
(38) Gu, J.; Leszczynski, J. *J. Phys. Chem. A* **2000**, *104*, 1898−1904.
(39) Meyer, M.; Brandl, M.; Suhnel, J. *J. Phys. Chem. A* **2001**, *105*, 8223−8225.
(40) Meyer, M.; Steinke, T.; Brandl, M.; Suhnel, J. *J. Comput. Chem*. **2001**, *22*, 109−124.
(41) Meyer, M.; Schneider, C.; Brandl, M.; Suhnel, J. *J. Phys. Chem. A* **2001**, *105*, 11560−11573.
(42) Gu. J.; Leszczynski, J.; Bansal, M. *Chem. Phys. Lett.* **1999**, *311*, 209−214.
(43) Gu. J.; Leszczynski, J. *J. Phys. Chem. A* **2000**, *104*, 6308−6313.
(44) Gu. J.; Leszczynski, J. *J. Phys. Chem. A* **2002**, *106*, 529−532.
(45) Gu, J.; Leszczynski, J. *J. Phys. Chem. A* **2000**, *104*, 7353−7358.
(46) Gu, J.; Leszczynski, J. *J. Phys. Chem. A* **2001**, *105*, 10366−10371.
(47) Gu, J.; Leszczynski, J. *Chem. Phys. Lett.* **2001**, *335*, 465−474.
(48) Gu, J.; Leszczynski, J. *Chem. Phys. Lett.* **2002**, *351*, 403−409.
(49) Meyer, M.; Sühnel, J. In *Computational Chemistry: Reviews of Current Trends*, Vol. 8; Leszczynski, J., Ed.; World Scientific: Singapore, 2003.
(50) Becke, A. D. *J. Chem. Phys.* **1993**, *98*, 5648−5652.
(51) Lee, C.; Yang W.; Parr, R. G. *Phys. Rev. B* **1988**, *37*, 785−789.
(52) Miehlich, B.; Savin, A.; Stoll H.; Preuss, H. *Chem. Phys. Lett*. **1989**, *157*, 200−206.
(53) Hehre, W. J.; Radom, L.; Schleyer, P. R.; Pople, J. A. *Ab Initio Molecular Orbital Theory*; Wiley: New York, 1986.
(54) Mebel, A. M.; Morokuma, K.; Lin, C. M. *J. Chem. Phys*. **1995**, *103*, 7414−7421.
(55) Johnson, B. G.; Gill, P. M. W.; Pople, J. A. *J. Chem. Phys*. **1993**, *98*, 5612−5626.
(56) Sponer, J.; Leszczynski, J.; Hobza, P. *J. Phys. Chem*. **1996**, *100*, 1965−1974.
(57) Gu, J.; Leszczynski, J. *J. Phys. Chem. A* **1999**, *103*, 577−584.
(58) Bader, R. F. W. *Atoms in Molecules: A Quantum Theory*; Clarendon Press: Oxford, U.K., 1990.
(59) Bader, R. F. W. *Chem. Rev.* **1991**, *91*, 893−928.
(60) Becke, A. D.; Edgecombe, K. E. *J. Chem. Phys*. **1990**, *92*, 5397−5403.
(61) Silvi, B.; Savin, A. *Nature* **1994**, *371*, 683−686.
(62) Frisch, M. J.; Trucks, G. W.; Schlegel, H. B.; Gill, P. M. W.; Johnson, B. G.; Robb, M. A.; Cheeseman, J. R.; Keith, T.; Petersson, G. A.; Montgomery, J. A.; Raghavachari, K.; Al-Laham, M. A.; Zakrzewski, V. G.; Ortiz, J. V.; Foresman, J. B.; Cioslowski, J.; Stefanov, B. B.; Nanayakkara, A.; Challacombe, M.; Peng, C. Y.; Ayala, P. Y.; Chen, W.; Wong, M. W.; Andres, J. L.; Replogle, E. S.; Gomperts, R.; Martin, R. L.; Fox, D. J.; Binkley, J. S.; Defrees, D. J.; Baker, J.; Stewart, J. P.; Head-Gordon, M.; Gonzalez, C.; Pople, J. A. *Gaussian 98*, Revision D.3; Gaussian, Inc.: Pittsburgh PA, 1998.
(63) Noury, S.; Krokidis, X.; Fuster, F.; Silvi, B. *TopMoD Package*; Universite Pierre et Marie Curie: Paris, France, 1997.
(64) Pauling, L. *The Nature of the Chemical Bond*, 3rd ed.; Cornell University Press: Ithaca, NY, 1960.
(65) Louit, G.; Hoquet, A.; Ghomi, M.; Meyer, M.; Sühnel J. *PhysChemComm* **2003**, *6*, 1−5.
(66) Louit, G.; Hoquet, A.; Ghomi, M.; Meyer, M.; Sühnel, J. *PhysChemComm* **2002**, *5*, 94−98.
(67) Popelier, P. L. A. *J. Phys. Chem. A* **1998**, *102*, 1873−1878.
(68) Vanquickenborne, L. G. Quantum Chemistry of Hydrogen Bond. In *Intermolecular Forces*; Huyskens, P. L., Luck, W. A. P., Zeegers-Huyskens, T., Eds.; Springer-Verlag: Berlin, Heidelberg, Germany, 1991; p 41.